

## Article (refereed) - postprint

---

Zhang, Xiuming; Wu, Yiyun; Liu, Xuejun; Reis, Stefan; Jin, Jiaxin; Dragosits, Ulrike; Van Damme, Martin; Clarisse, Lieven; Whitburn, Simon; Coheur, Pierre-Francois; Gu, Baojing. 2017. **Ammonia emissions may be substantially underestimated in China.** *Environmental Science & Technology*, 51 (21). 12089-12096. <https://doi.org/10.1021/acs.est.7b02171>

© 2017 American Chemical Society

This version available <http://nora.nerc.ac.uk/518058/>

NERC has developed NORA to enable users to access research outputs wholly or partially funded by NERC. Copyright and other rights for material on this site are retained by the rights owners. Users should read the terms and conditions of use of this material at <http://nora.nerc.ac.uk/policies.html#access>

**This document is the final manuscript version of the journal article, incorporating any revisions agreed during the peer review process. There may be differences between this and the publisher's version. You are advised to consult the publisher's version if you wish to cite from this article.**

The definitive version is available at <http://pubs.acs.org/>

Contact CEH NORA team at  
[noraceh@ceh.ac.uk](mailto:noraceh@ceh.ac.uk)

**Ammonia emissions may be substantially underestimated in China**

Xiuming Zhang<sup>†,‡</sup>, Yiyun Wu<sup>‡</sup>, Xuejun Liu<sup>§</sup>, Stefan Reis<sup>#,‡</sup>, Jiaxin Jin<sup>¶</sup>, Ulrike Dragosits<sup>#</sup>, Martin Van Damme<sup>Δ</sup>, Lieven Clarisse<sup>Δ</sup>, Simon Whitburn<sup>Δ</sup>, Pierre-François Coheur<sup>Δ</sup>, Baojing Gu<sup>†,Φ,⊥,\*</sup>

<sup>†</sup>Department of Land Management, Zhejiang University, Hangzhou 310058, People's Republic of China;

<sup>‡</sup>Policy Simulation Laboratory, Zhejiang University, Hangzhou 310058, People's Republic of China;

<sup>§</sup>College of Resources and Environmental Sciences, China Agricultural University, Beijing 100193, People's Republic of China;

<sup>#</sup>NERC Centre for Ecology & Hydrology, Bush Estate, Penicuik, Midlothian, EH260QB, United Kingdom;

<sup>‡</sup>University of Exeter Medical School, Knowledge Spa, Truro, TR1 3HD, United Kingdom;

<sup>¶</sup>International institute for earth system science, Nanjing University, Nanjing 210046, People's Republic of China;

<sup>Δ</sup>Université libre de Bruxelles (ULB), Atmospheric Spectroscopy, Service de Chimie Quantique et Photophysique CP 160/09, Avenue F.D. Roosevelt 50, 1050 Bruxelles, Belgium

<sup>Φ</sup>School of Agriculture and Food, The University of Melbourne, Victoria 3010, Australia

<sup>⊥</sup>Laboratory of Rural-Urban Construction Land Economical and Intensive Use, Ministry of Land and Resources, Beijing 100812, China

**\*Corresponding Author:**

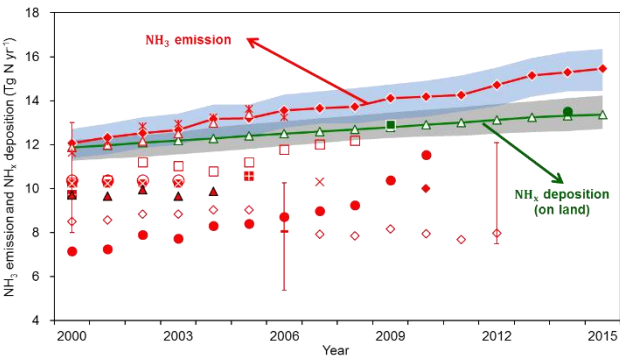
Department of Land Management, Zhejiang University, Zijingang Campus, 866 Yuhangtang Road, Hangzhou 310058, PR China. Tel & Fax: +86 571 8898 2615. E-mail: [bjgu@zju.edu.cn](mailto:bjgu@zju.edu.cn)

**Abstract**

China is a global hotspot of atmospheric ammonia ( $\text{NH}_3$ ) emissions and, as a consequence, very high nitrogen (N) deposition levels are documented. However, previous estimates of total  $\text{NH}_3$  emissions in China were much lower than inference from observed deposition values would suggest, highlighting the need for further investigation. Here, we reevaluated  $\text{NH}_3$  emissions based on a mass balance approach, validated by N deposition monitoring and satellite observations, for China for the period of 2000 to 2015. Total  $\text{NH}_3$  emissions in China increased from  $12.1 \pm 0.8 \text{ Tg N yr}^{-1}$  in 2000 to  $15.6 \pm 0.9 \text{ Tg N yr}^{-1}$  in 2015 at an annual rate of 1.9%, which is approximately 40% higher than existing studies suggested. This difference is mainly due to more emission sources now having been included and  $\text{NH}_3$  emission rates from mineral fertilizer application and livestock having been underestimated previously. Our estimated  $\text{NH}_3$  emission levels are consistent with the measured deposition of  $\text{NH}_x$  (including  $\text{NH}_4^+$  and  $\text{NH}_3$ ) on land (11-14  $\text{Tg N yr}^{-1}$ ) and the substantial increases in  $\text{NH}_3$  concentrations observed by satellite measurements over China. These findings substantially improve our understanding on  $\text{NH}_3$  emissions, implying that future air pollution control strategies have to consider the potentials of reducing  $\text{NH}_3$  emission in China.

**Keywords:** fertilizer; nitrogen deposition; mass balance; satellite measurements; agriculture; temperature

TOC Art



## INTRODUCTION

Nitrogen (N) plays an important role in all living systems and their environment.<sup>1, 2</sup> Reactive N ( $N_r$ ) released to the environment is dispersed by atmospheric and hydrologic transport processes and can accumulate in air, soils, vegetation, and groundwater.<sup>1</sup> Almost all emitted  $N_r$  in the forms of nitrogen oxides ( $NO_x$ , defined as the sum of all species that contained oxidized nitrogen) and ammonia ( $NH_3$ ) is transferred back to the Earth's surface within hours to days of its release.<sup>2</sup>  $NH_3$  emitted to the atmosphere is either deposited directly or transformed into an ammonium aerosol (e.g., ammonium nitrates and ammonium sulfate) often transported over long distances.<sup>3</sup> Two types of  $NH_x$  ( $NH_3$  (gas) +  $NH_4^+$  (aerosol)) deposition usually occur: dry deposition of  $NH_3$  close to the emission sources,<sup>4, 5</sup> and wet deposition of  $NH_4^+$  that can occur at far distances downwind from the sources.<sup>6</sup> N biogeochemical cycles follow the principle of mass balance, and the  $N_r$  input to and output from the atmosphere system are normally balanced.<sup>7</sup> Therefore,  $NH_x$  deposition fluxes are closely related to  $NH_3$  emissions. Galloway et al.<sup>8</sup> and Fowler et al.<sup>2</sup> elaborated the process of global N cycling and estimated that global  $NH_3$  emissions and  $NH_x$  deposition are in balance (Table 1). Global  $NH_x$  deposition depends strongly on total  $NH_3$  emissions, with the spatial distribution of emissions and atmospheric transport pathways affecting the downwind deposition fluxes to the oceans.<sup>9</sup>

Mainland China has long coastlines (total length about 18 000 km), bordering the Northwestern Pacific Ocean, which is primarily located downwind of emission sources on the Asian continent.<sup>10</sup> As a consequence, long-range transport will lead to a share of ammonium aerosols being deposited outside of China's land area, because prevailing wind directions and river catchment flows of China result in pollutants being carried from China to the North Pacific Ocean.<sup>11-13</sup> Figure S1 illustrates the sources and fates of  $NH_3$  in China. It is noticeable that the Tibetan Plateau blocks most pollutant transfer into China from other countries in the west such as India though some evidence has emerged of transport of air pollutants across the Himalayas.<sup>14, 15</sup> China receives little  $NH_x$  from other countries through atmospheric circulation, but transports  $N_r$  to surrounding marine ecosystems, and is overall a net exporter of  $NH_x$  deposition.<sup>14</sup> Therefore, the flux of  $NH_x$  deposition on land could be used to constrain the spatial and temporal variations of  $NH_3$  emission in China.<sup>16</sup>

Over the past two decades, China has witnessed a substantial increase in  $N_r$  pollution and has been a global "hotspot" for both  $NH_3$  emissions and N deposition due to rapid increases in industrialization, urbanization and intensified agricultural production.<sup>7, 17, 18</sup> Rapid increases in atmospheric  $NH_3$  concentrations and the subsequent N depositions have various effects on ecosystems, such as soil acidification, water eutrophication, biodiversity loss and air pollution.<sup>19, 20</sup> Although many studies on emission inventories in general and  $NH_3$  emissions in particular have been conducted in China, large uncertainties and contradictory results were found in terms of spatial and temporal variations of  $NH_3$

emissions (e.g., Dong et al.<sup>21</sup>; Huang et al.<sup>22</sup>; Kang et al.<sup>23</sup>). Total estimates of NH<sub>3</sub> emissions available for China range from 7-8 Tg N yr<sup>-1</sup><sup>23,24</sup> to around 11-12 Tg N yr<sup>-1</sup>.<sup>25</sup>,<sup>26</sup> Some studies<sup>24, 26</sup> recorded an increasing trend, while other studies<sup>23</sup> argued a downward trend of total NH<sub>3</sub> emission in China for the recent decade. Previous studies rarely used other data apart from ground-based concentration measurements for emission verification, such as N deposition monitoring or satellite observation to calibrate estimates and validate NH<sub>3</sub> inventories.

Recent studies have addressed the important role of NH<sub>3</sub> in the formation of fine particles (PM<sub>2.5</sub>) in China,<sup>27, 28</sup> putting more of an emphasis on the need to refine and better quantify NH<sub>3</sub> emissions and their contribution to air pollution, including for urban areas, in China. Thus, in this paper we aimed to (i) advance our understanding by designing a systematic framework for the analysis of NH<sub>3</sub> sources, emissions, and environmental fates in China; (ii) review and revise the NH<sub>3</sub> emission inventory from 2000 to 2015 in China with a mass balance approach; and (iii) evaluate the uncertainties attributed to NH<sub>3</sub> emissions by validation of NH<sub>x</sub> deposition and satellite measurements.

## METHODS

**Datasets.** This study covers the entire land area of mainland China; Taiwan, Hong Kong, and Macao were excluded owing to data limitations. Data used in this study can be divided into two categories: (i) summary information for China such as population, GDP, land use, fertilizer use, crop/livestock production, and energy consumption in different sectors, all taken from the national data center<sup>29</sup> and FAO statistics<sup>30</sup>; (ii) parameters and coefficients used for the calculation of NH<sub>3</sub>-N fluxes, both obtained from synthesis of peer-reviewed literature and field measurements. We established multiple datasets for the calculation of NH<sub>x</sub> emissions from 2000 to 2015 in China on a provincial scale. Note that all the units of NH<sub>x</sub> fluxes have been converted to Tg N yr<sup>-1</sup>. Details about the selection criteria applied to and parameters and coefficients can be found in SI methods.

**Model Description.** We used the Coupled Human And Natural Systems (CHANS) model to quantify NH<sub>3</sub> fluxes within China. The CHANS model incorporates and integrates all N<sub>r</sub> fluxes and their interactions that can be identified, together with the linkages among subsystems (Figure S2). The basic principle of the CHANS model is mass balance for the whole system and each subsystem. A detailed description of CHANS can be found in Gu et al.<sup>31</sup> In this study, we focus on the atmosphere subsystem (AT) which receives NH<sub>3</sub> input from 13 subsystems and deposits NH<sub>x</sub> to land subsystems. In addition, it can also transfer NH<sub>x</sub> to or receive NH<sub>x</sub> from other countries/oceans through atmospheric circulation. The input of NH<sub>3</sub> is either larger or equal to the output of NH<sub>x</sub>. A summary of the main source categories comprised in the NH<sub>3</sub> emission inventory is listed in Table S1.

Meteorological conditions strongly influence the rate of NH<sub>3</sub> emissions.<sup>32, 33</sup> We

quantitatively estimate the impacts of climate change on  $\text{NH}_3$  emission based on the climate-dependent paradigm developed by Sutton et al.<sup>32</sup> This climate-dependent paradigm is generally universal among regions, and can be used in China. In principle, according to solubility and dissociation thermodynamics,  $\text{NH}_3$  volatilization potential nearly doubles for an increase of temperature by  $5^\circ\text{C}$ , equivalent to a  $Q_{10}$  (the relative increase over a range of  $10^\circ\text{C}$ ) of 1–4.<sup>32</sup> Note that in this study, we only consider the temperature-dependence effect on agricultural sources given that to date only few studies have emerged in literature which thoroughly quantify the effect of temperature on non-agricultural sectors.<sup>34</sup> Base on Sutton et al.,<sup>32</sup> an average  $Q_{10}$  of 2 was used for  $\text{NH}_3$  EFs from fertilizer application across China; an average  $Q_{10}$  of 1.25 was used for  $\text{NH}_3$  EFs from pigs, sows, poultry, rabbits, sheep and goats while an average  $Q_{10}$  of 2.5 for cattle, horses, donkeys, mules. Prior to the calibration of temperature-dependence effects, we have summarized the average  $\text{NH}_3$  EFs using correction coefficients for various factors. Details on the approach can be found in SI text.

The annual average temperature for fifteen years (2000–2015) at  $9.7^\circ\text{C}$  across China has been selected as a reference temperature and warmer or colder annual averages as a proxy for calibration of the  $\text{NH}_3$  emission. The calculation principles are as follow:

$$AT_{IN} = \sum_{i=1}^{13} E_{Item,i} + AT_{IN_{Import}} \quad (1)$$

$$E_{Item,i,j} = \sum_p EF_{i,j,p} \times f(T_{j,p}) \times AL_{i,j,p} \quad (2)$$

$$f(T_{j,p}) = \frac{(Q_{10,j,p}-1)}{10} \times (T_j - T_0) + 1 \quad (3)$$

$$AT_{OUT} = AT_{OUT_{Dep}} + AT_{OUT_{Export}} \quad (4)$$

$$AT_{IN} \geq AT_{OUT} \quad (5)$$

where  $AT_{IN}$  and  $AT_{OUT}$  are the total  $\text{NH}_x$  input to and output from atmosphere subsystem;  $E_{Item,i,j}$  is the  $\text{NH}_x$  emission from other 13 subsystems to atmosphere;  $i, j$  and  $p$  represent the subsystem, the year and the source type, respectively;  $EF_{i,j,p}$  is the corresponding emission factor (EF);  $f(T_{j,p})$  represents a function of climate effect on  $\text{NH}_3$  emission;  $T_j$  is the annual average temperature ( $^\circ\text{C}$ ),  $T_0$  represents the fifteen years (2000–2015) average temperature ( $9.7^\circ\text{C}$ );  $Q_{10,j,p}$  stands for a temperature effect on the  $\text{NH}_3$  volatilization potential;  $AL_{i,j,p}$  is the activity data;  $AT_{OUT_{Dep}}$  is the  $\text{NH}_x$  deposition on land, including both dry and wet deposition.  $AT_{OUT_{Export}}$  is the  $\text{NH}_x$  transferred to surrounding areas (mainly to ocean) through atmospheric circulation that advects  $\text{NH}_x$  away from China.

**Uncertainty analysis.** Monte Carlo simulation was used to quantify the variability of the  $\text{NH}_3$  fluxes. In Monte Carlo simulations, random numbers are selected from the normal or uniform distribution of input variables and a variation range is attributed to the emission inventory. In order to thoroughly test the accuracy of the simulation results, 10,000 Monte Carlo simulations were executed to estimate the range of  $\text{NH}_3$  emission

uncertainties for different sources. Meanwhile, the mass balance approach used in the CHANS model constrains the uncertainty ranges and helps to refine the overall uncertainty.<sup>7</sup> Details about the uncertainty assessment can be found in the SI text and tables.

## RESULTS

**Total NH<sub>3</sub> emission in 2015.** The total NH<sub>3</sub> emission into the atmosphere was estimated at 15.6±0.9 Tg N in 2015 for China. Agricultural sources were the largest contributors (13.6±0.8 Tg N), accounting for 88% of total NH<sub>3</sub> emissions, with 5.8±0.3 Tg N and 6.6±0.5 Tg N stemming from cropland and livestock, respectively. The majority of the NH<sub>3</sub> emissions from cropland originated from the application of mineral fertilizers (5.4±0.2 Tg N), and the rest from irrigation, agricultural soils, N-fixing crops, and composting of crop residues (Figure S3). An estimated 3.8±0.2 Tg N was emitted from livestock housing and manure storage. In addition, 2.8±0.3 Tg N was emitted from manure application to cropland, which in some studies has been attributed to cropland emissions.<sup>35, 36</sup>

The spatial distribution of NH<sub>3</sub> emissions on a provincial scale in 2015 is shown in Figure 1a, revealing a strong spatial variability and association with the distribution of arable land. High NH<sub>3</sub> emission densities above 50 kg N ha<sup>-1</sup> were concentrated across the North China Plain, where intensive agriculture for both crop production and animal husbandry are located. Sichuan Basin, Middle South China and Northeastern China also show high NH<sub>3</sub> emission densities. In contrast, low NH<sub>3</sub> emission densities of less than 10 kg N ha<sup>-1</sup> were primarily found across western China, e.g. Tibet, Qinghai, Inner Mongolia and Gansu, which are characterized by dry regions with low agricultural production and little N fertilizer use.<sup>29</sup>

**Temporal trends of NH<sub>3</sub> emissions.** Total NH<sub>3</sub> emissions increased from 12.1±0.8 Tg N in 2000 to about 15.6±0.9 Tg N in 2015 with an annual rate of 1.9% (statistically significant). ~85% of the inter-annual variations could be well explained by the changes of human activity levels (Figure S4), and the remaining 15% were attributed to air temperature changes during this period (Figure S5). Agriculture is the main emission source, accounting for ~87% of the total NH<sub>3</sub> emission in China, with on average, 43.1% (41.6-44.1%) contributed by livestock manure and 36.4% (35.0-38.3%) by fertilizer application. Non-agricultural sources account for only about 13% of total national NH<sub>3</sub> emissions, including humans responsible for 6.6% (5.1-8.8%), other sources (fuel combustion, waste disposal, traffic sources, chemical industry, urban green land) contributed to less than 2% (Figure S4).

**Uncertainty assessment.** The range of NH<sub>3</sub> emissions with a 95% confidence interval for 2000, 2005, 2010, 2015 was estimated at 11.4-12.7, 12.3-13.8, 13.3-14.9, and 14.5-16.6 Tg N yr<sup>-1</sup>, respectively (Figure 2). Uncertainty contribution and variation ranges of

different emission source sectors are presented in Table S14. Livestock manure and fertilizer application were identified as the key sources, with contributions to overall uncertainty of 43.1% and 36.4%, respectively.

## DISCUSSION

**Validation by  $\text{NH}_x$  deposition.** In contrast to the bottom-up estimates of  $\text{NH}_3$  emission in current inventories,  $\text{NH}_x$  deposition can be comparatively well constrained based on data from field monitoring. Based on our  $\text{NH}_3$  emission estimations, we could derive the range of  $\text{NH}_x$  deposition in mainland China ( $\text{Dep}_{\text{derived}} = \text{NH}_3 \text{ emission} - \text{exported} + \text{imported}$ , where exported  $\text{NH}_3$  flux accounts for ~20% of  $\text{NH}_3$  emission<sup>14</sup>, and imported N flux from outside contributed by foreign anthropogenic emissions is ~1 Tg N yr<sup>-1</sup><sup>10</sup>). The derived  $\text{NH}_x$  deposition was calculated at 12.6 Tg N in 2010 (Figure 2).

To be directly comparable with the observation data of  $\text{NH}_x$  deposition, Figure 2 integrated the  $\text{NH}_x$  deposition on land for China (data extracted from Liu et al.<sup>17</sup> and Xu et al.<sup>6</sup>). Liu et al.<sup>17</sup> and Xu et al.<sup>6</sup> conducted a comprehensive evaluation of N deposition dynamics across China (Figure S6) based on a Nationwide Nitrogen Deposition Monitoring Network (NNDMN). Result indicated a  $\text{NH}_x$  deposition around 11-14 Tg N yr<sup>-1</sup> over land areas in China during 2000-2015, with a 12.9 Tg N in 2010. A range of additional studies based on N deposition monitoring data also support the estimated range of  $\text{NH}_x$  deposition over China (Table 2). Therefore, the derived  $\text{NH}_x$  deposition from our estimate of  $\text{NH}_3$  emission agreed well with the observed  $\text{NH}_x$  deposition over land areas in China.

It is noticeable from Figure 2 that the difference between  $\text{NH}_3$  emissions and terrestrial  $\text{NH}_x$  deposition increased in recent years. We assume that this can be attributed to the increased long-distance transport of  $\text{NH}_x$  deposition to the ocean. Elevated  $\text{NH}_x$  deposition rates found in the North and Northwestern Pacific Oceans<sup>11, 13</sup> demonstrates that the formation of ammonium sulphate and -nitrate extended the lifetime of  $\text{NH}_3$  in the atmosphere, promoting its long-range transport to ocean.<sup>10</sup> This is in line with the observation that, despite the most recent reductions of  $\text{NO}_x$  and  $\text{SO}_2$  emissions<sup>37</sup> in China, the molar amount of ( $2\text{SO}_2 + \text{NO}_x$ ) still substantially exceeded that of  $\text{NH}_3$  at least until 2015 (Figure 3), suggesting that  $\text{NH}_3$  emissions presented the limiting factor to the formation of ammonium aerosols. Thus, the increase of  $\text{NH}_3$  emission would increase the formation of ammonium aerosols and the long-range transport to ocean during 2000-2015 in China. It should be noted that while Figure 3 presents a mass balance limit to the relative components of each species, other factors, i.e. temperature, relative humidity, and aerosol composition could affect the limitations of aerosol formation,<sup>27</sup> and a full atmospheric chemistry transport model assessment would be needed to further assess limiting reagents.

**Validation by satellite observations.** Ground-based measurements of ambient  $\text{NH}_3$  are

sparse and not always representative for a larger area. Satellites provide an alternative and are ideal to measure  $\text{NH}_3$  spatial and temporal variability on global scale.<sup>38, 39</sup> Figure 1 presents the spatial distributions of  $\text{NH}_3$  emission and the  $\text{NH}_3$  vertical column densities (VCDs) measured with the Infrared Atmospheric Sounding Interferometer (IASI) satellite for 2015 over China.<sup>40</sup> The spatial variability of our estimates of the  $\text{NH}_3$  emission densities agree well with the IASI- $\text{NH}_3$  VCDs distribution, with the largest  $\text{NH}_3$  emission density found in the North China Plain, Sichuan Basin and Northeastern China. Relatively high  $\text{NH}_3$  VCDs could also be observed in Xinjiang by satellite IASI instrument, which is not captured by our emission map. There is little emission of  $\text{SO}_2$  and  $\text{NO}_x$  from industrial sources in Xinjiang compared to that in Eastern China.<sup>41</sup> Therefore, a reduced conversion rate to aerosol is expected. This, and the dry climate is probably responsible for a longer lifetime of  $\text{NH}_3$  in the atmosphere in Xinjiang compared to other regions in China. This will lead, in those regions to a larger buildup of  $\text{NH}_3$ , and hence larger observed columns and a larger qualitative discrepancy with the emission inventory.

Recently, Warner et al.<sup>33</sup> showed an increasing trend of  $\text{NH}_3$  VCDs in China from 2003 to 2015 with an increment of  $0.076 \pm 0.020$  ppbv (parts-per-billion by volume) per year ( $2.3\% \text{ yr}^{-1}$ ) using measurements of the Atmospheric InfraRed Souder (AIRS) satellite. This increasing trend of  $\text{NH}_3$  VCDs in China agreed well with our results that showed an annual increase rate of  $2.0\%$  during the same period. Generally, the increased  $\text{NH}_3$  emissions contributed to the variation in  $\text{NH}_3$  VCDs. It suggested that the decreasing trends or trends with turning points of  $\text{NH}_3$  emission from 2000 to 2015 found in previous studies are not accurate (Figure 2). For instance, a recent study by Kang et al.<sup>23</sup> estimated that total  $\text{NH}_3$  emissions in China showed a downward trend from  $8.5 \text{ Tg N}$  in 2000 to  $8.0 \text{ Tg N}$  in 2012, contradictory to the increasing trend found in satellite measurements. However, note that satellite concentrations should not be directly compared with emissions, as  $\text{NH}_3$  columns are in addition to sources, determined by transport and sinks<sup>40, 41</sup>. Hence, we suggest such data is primarily used for qualitative comparisons such as temporal trend analysis.

**Comparison with other studies.** Figure 2 indicates that our results estimated  $\text{NH}_3$  emissions to be about 40% higher than previous studies suggested, majority of which estimated a lower amount of  $\text{NH}_3$  emission than inference from observed  $\text{NH}_x$  deposition would yield. Table 3 shows a quantitative comparison with previous studies from five main sources, and the differences are mainly arising from estimates of emissions from fertilizer use and livestock production. In addition, we included additional emission sources compared to other studies, such as grassland, aquaculture, traffic sources, urban vegetation, humans and pets, even though the latter contributed a relatively small proportion of total emissions (SI text).

The total amount of mineral fertilizer applied and emission factors (EFs) for  $\text{NH}_3$  volatilization are two key factors that directly affect  $\text{NH}_3$  emissions from N fertilizer

application. Compared to other studies, the difference regarding estimated activity data (i.e. amount of fertilizer uses) is less than 5%. However, the final corrected EFs (16.2–18.4%, average 17.0%) used in this study were about 16.6% higher than those used in other studies (Figure S10, average 14.6%). The majority of previous inventories compiled for China used constant European-based emission factors (EFs) (e.g., Dong et al.<sup>21</sup>; Kang et al.<sup>23</sup>), and did not adjust for specific agricultural practices, environmental conditions and climatological factors. Some studies<sup>23, 42</sup> adopted much lower EFs (Figure S10, average 12.8%) because they believed that an anticipated shift of dominant fertilizer types from ABC to urea would substantially reduce the NH<sub>3</sub> emission.<sup>23, 42</sup> In fact, the actual EFs are substantially influenced by the method of fertilizer application used. ABC is normally applied as base fertilizer with deep placement that results in a lower EF, while urea is widely used for top-dressing and surface application<sup>43, 44</sup>. The percentage of topdressing for urea is higher than that for ABC (Table S5) and as such is likely to substantially increase NH<sub>3</sub> emissions in China.<sup>44</sup> Therefore, the gradual shift of fertilizer type from ABC to urea would not significantly change the overall NH<sub>3</sub> EF for fertilizer application in China.

A recent meta-analysis<sup>45</sup> on the topic of NH<sub>3</sub> volatilization from global fertilizer use indicates that the global average percentage of N lost as NH<sub>3</sub> was 17.6%. The NH<sub>3</sub> volatilization rate for China is expected to be higher than this value, given its higher application rate and lower N use efficiency considering the fact that most farming is done on smallholder farms, which rely mainly on family labor and are traditionally slow to adapt technical improvements such as 4R fertilization management.<sup>46</sup>

Table 3 indicates that the total NH<sub>3</sub> emissions from livestock calculated in this study were 1.4 Tg N yr<sup>-1</sup> higher than other studies on average, such as REAS2.1,<sup>26</sup> Xu et al.<sup>35</sup> and EDGARv4.3.1.<sup>24</sup> The EFs for livestock used in this study are compared with other studies in Figure S6. In fact, due to the absence of closed systems to produce liquid manure, the air-dry process used to produce manure for field application in China results in high emissions of NH<sub>3</sub> from livestock production.<sup>47</sup> In addition, the backyard and small-scale livestock farms still dominate animal production in China, which is difficult to supervise the NH<sub>3</sub> emission from livestock production and further introduce advanced technologies to reduce the NH<sub>3</sub> emission due to high costs.<sup>47</sup> Therefore, even assuming the same excretion rate for livestock, the resulting NH<sub>3</sub> emission rate is expected to be higher in China because manure management systems are not as advanced as developed countries.

**Uncertainty and Limitation.** To estimate the uncertainty range on a national scale is challenging given the large spatial variability of EFs of NH<sub>3</sub>. A simple additive approach for all uncertainties from each region and source would undoubtedly exaggerate the overall uncertainty. The NH<sub>3</sub> emissions in this study were calculated based on a full life-cycle analysis, which is a framework to quantify and track the trajectory of all nitrogen

fluxes in the CHANS.<sup>7,31</sup> Thus, the uncertainty range inherent to the CHANS model could be well constrained by the mass balance calculation in all the 13 subsystems, combining with Monte Carlo simulations.

However, we have identified several limitations of this study, especially for the major emission sources of N fertilizer and livestock. The actual EFs for fertilizer application are substantially influenced by many parameters, including meteorological conditions, soil properties, fertilizer application methods, application rate, fertilizer type and so on.<sup>48</sup> However, generating a matching dataset of human activities data (e.g., N fertilizer application rate) with the same degree of detail and resolution on national scale is outside the scope of this study. At the same time, the influence of these factors on NH<sub>3</sub> emission at a large scale has not yet been well studied and quantified, to our knowledge. Therefore, it is difficult to integrate all the factors into the CHANS and comprehensively quantify the effects of those factors. Future work to build comprehensive datasets including both spatial and temporal variations of the key influencing factors would help to refine the results.

In addition, we assume there is no significant inter-annual change in the percentage of intensive rearing systems, manure management practice which is typically affected by many factors, including the housing structure, manure storage system, spreading technique, and so on.<sup>49</sup> However, manure management practices in China have been subject to great changes over the time period of 2000-2015,<sup>29</sup> hence additional uncertainties may be introduced due to using constant parameters for livestock manure during the study period<sup>23</sup>.

Some uncertainties may still exist in the observed NH<sub>x</sub> deposition used in this study due to the relatively limited number of sampling sites. In addition, NH<sub>3</sub> deposition may be overestimated at rural sites with relatively high canopy compensation points as a result of fertilized croplands or vegetation<sup>6</sup>. Furthermore, there may also be large uncertainties arising from comparison with satellite data, because observed differences between ammonia emission and NH<sub>3</sub> VCDs remain unclear to some extent, for instance, in locations such as Xinjiang. These uncertainties may affect the validation of NH<sub>3</sub> emissions in this paper.

**Outlook.** Refining the NH<sub>3</sub> emission inventory datasets with high spatiotemporal resolution is crucial for the assessment of future policy implications with regard to mitigation options. This paper highlights that the overall amount of NH<sub>3</sub> emissions may be substantially underestimated in China (Figure 2). However, we still lack a substantial amount of information on spatial resolution at regional to local scales, as well as future changes, which are decision making. Further work is still required to increase the reliability and accuracy of NH<sub>3</sub> emission inventory datasets, underpinned by high-resolution observations, process-based experiments and model-data assimilation to fully quantify more realistic NH<sub>3</sub> emissions. This can enhance our understanding on the variation of NH<sub>3</sub> emission and its driving forces.

Furthermore, NH<sub>3</sub> plays a crucial role in the formation of secondary inorganic aerosols (SIAs) that are the predominant components of fine particles in China.<sup>20</sup>

However, until now no control strategies have yet been implemented for NH<sub>3</sub> emissions in China. Effective strategies for the reduction of NH<sub>3</sub> emissions in China are thus urgently needed given a 40% higher NH<sub>3</sub> emission than previous thoughts. In support of such strategies, a comprehensive and accurate NH<sub>3</sub> emission inventory is also vital to future air pollution prevention and control in China, which can be integrated into air quality model and serve as a baseline toward tracking emission trends, developing mitigation strategies, and assessing progress.

### Acknowledgments

This work was supported in part by the National Key Research and Development Project of China (2016YFC0207906); National Natural Science Foundation of China (No. 41773068 and 41425007); the Fundamental Research Funds for the Central Universities (No. 581280\*172220261/010); the Open Fund of Key Laboratory of Nonpoint Source Pollution Control, Ministry of Agriculture, China (1610132016005); the Discovery Early Career Researcher Award by the Australian Research Council (DE170100423); and the Newton Fund via UK BBSRC/NERC (BB/N013484/1) for the UK-China Virtual Joint Centre on Nitrogen “N-Circle”.

### Note

The authors declare no competing financial interest.

### Supporting Information Available

The Supporting Information includes is available free of charge on the ACS Publications website.  
Text S1–4, Table S1–16 and Figure S1–9 (PDF).

## REFERENCES

- (1) Galloway, J. N.; Townsend, A. R.; Erisman, J. W.; Bekunda, M.; Cai, Z.; Freney, J. R.; Martinelli, L. A.; Seitzinger, S. P.; Sutton, M. A. Transformation of the Nitrogen Cycle: Recent Trends, Questions, and Potential Solutions. *Science* **2008**, *320* (5878), 889-892.
- (2) Fowler, D.; Coyle, M.; Skiba, U.; Sutton, M. A.; Cape, J. N.; Reis, S.; Sheppard, L. J.; Jenkins, A.; Grizzetti, B.; Galloway, J. N.; et al. The global nitrogen cycle in the twenty-first century. *Philos. Trans. R. Soc., B* **2013**, *368* (1621), 20130164.
- (3) Kirkby, J.; Curtius, J.; Almeida, J.; Dunne, E.; Duplissy, J.; Ehrhart, S.; Franchin, A.; Gagné, S.; Ickes, L.; Kürten, A.; et al. Role of sulphuric acid, ammonia and galactic cosmic rays in atmospheric aerosol nucleation. *Nature* **2011**, *476* (7361), 429-433.
- (4) Vogt, E.; Dragosits, U.; Braban, C. F.; Theobald, M. R.; Dore, A. J.; van Dijk, N.; Tang, Y. S.; McDonald, C.; Murray, S.; Rees, R. M.; et al. Heterogeneity of atmospheric ammonia at the landscape scale and consequences for environmental impact assessment. *Environ. Pollut.* **2013**, *179* (8), 120-131.
- (5) Dragosits, U.; Theobald, M. R.; Place, C. J.; Lord, E.; Webb, J.; Hill, J.; ApSimon, H. M.; Sutton, M.

- 412 A. Ammonia emission, deposition and impact assessment at the field scale: a case study of sub-grid spatial  
413 variability. *Environ. Pollut.* **2002**, *117* (1), 147-158.
- 414 (6) Xu, W.; Luo, X. S.; Pan, Y. P.; Zhang, L.; Tang, A. H.; Shen, J. L.; Zhang, Y.; Li, K. H.; Wu, Q. H.;  
415 Yang, D. W.; et al. Quantifying atmospheric nitrogen deposition through a nationwide monitoring network  
416 across China. *Atmos. Chem. Phys.* **2015**, *15* (21), 12345-12360.
- 417 (7) Gu, B.; Ju, X.; Chang, J.; Ge, Y.; Vitousek, P. M. Integrated reactive nitrogen budgets and future trends  
418 in China. *Proc. Natl. Acad. Sci. U. S. A.* **2015**, *112* (28), 8792-8797.
- 419 (8) Galloway, J. N.; Dentener, F. J.; Capone, D. G.; Boyer, E. W.; Howarth, R. W.; Seitzinger, S. P.; Asner,  
420 G. P.; Cleveland, C. C.; Green, P. A.; Holland, E. A.; et al. Nitrogen cycles: past, present, and future.  
421 *Biogeochemistry* **2004**, *70* (2), 153-226.
- 422 (9) Doney, S. C.; Mahowald, N.; Lima, I.; Feely, R. A.; Mackenzie, F. T. Impact of anthropogenic  
423 atmospheric nitrogen and sulfur deposition on ocean acidification and the inorganic carbon system. *Proc.*  
424 *Natl. Acad. Sci. U. S. A.* **2007**, *104* (34), 14580-14585.
- 425 (10) Luo, X. S.; Tang, A. H.; Shi, K.; Wu, L. H.; Li, W. Q.; Shi, W. Q.; Shi, X. K.; Erisman, J. W.; Zhang,  
426 F. S.; Liu, X. J. Chinese coastal seas are facing heavy atmospheric nitrogen deposition. *Environ. Res. Lett.*  
427 **2014**, *2014* (9), 1-10.
- 428 (11) Kim, I.; Lee, K.; Gruber, N.; Karl, D. M.; Bullister, J. L.; Yang, S.; Kim, T. Increasing anthropogenic  
429 nitrogen in the North Pacific Ocean. *Science* **2014**, *346* (6213), 1100-1102.
- 430 (12) Zhao, Y.; Zhang, L.; Pan, Y.; Wang, Y.; Paulot, F.; Henze, D. K. Atmospheric nitrogen deposition to  
431 the northwestern Pacific: seasonal variation and source attribution. *Atmos. Chem. Phys.* **2015**, *15* (18),  
432 10905-10924.
- 433 (13) Kim, T.; Lee, K.; Najjar, R. G.; Jeong, H.; Jeong, H. J. Increasing N abundance in the Northwestern  
434 Pacific Ocean due to atmospheric nitrogen deposition. *Science* **2011**, *334* (6055), 505-509.
- 435 (14) Zhao, Y.; Zhang, L.; Chen, Y.; Liu, X.; Xu, W.; Pan, Y.; Duan, L. Atmospheric nitrogen deposition to  
436 China: A model analysis on nitrogen budget and critical load exceedance. *Atmos. Environ.* **2017**, *153*, 32-  
437 40.
- 438 (15) Zheng, J.; Hu, M.; Du, Z.; Shang, D.; Gong, Z.; Qin, Y.; Fang, J.; Gu, F.; Li, M.; Peng, J.; et al.  
439 Influence of biomass burning from South Asia at a high-altitude mountain receptor site in China. *Atmos.*  
440 *Chem. Phys.* **2017**, *17* (11), 6853-6864.
- 441 (16) Paulot, F.; Jacob, D. J.; Pinder, R. W.; Bash, J. O.; Travis, K.; Henze, D. K. Ammonia emissions in  
442 the United States, European Union, and China derived by high-resolution inversion of ammonium wet  
443 deposition data: Interpretation with a new agricultural emissions inventory (MASAGE\_NH<sub>3</sub>). *J. Geophys.*  
444 *Res. Atmos.* **2014**, *119* (7), 4343-4364.
- 445 (17) Liu, X.; Zhang, Y.; Han, W.; Tang, A.; Shen, J.; Cui, Z.; Vitousek, P.; Erisman, J. W.; Goulding, K.;  
446 Christie, P.; et al. Enhanced nitrogen deposition over China. *Nature* **2013**, *494* (7438), 459-462.
- 447 (18) Liu, L.; Zhang, X.; Wang, S.; Lu, X.; Ouyang, X. A review of spatial variation of inorganic nitrogen  
448 (N) wet deposition in China. *PLoS ONE* **2016**, *11* (1), e0146051.
- 449 (19) Hernández, D. L.; Vallano, D. M.; Zavaleta, E. S.; Tzankova, Z.; Pasari, J. R.; Weiss, S.; Selman, P.  
450 C.; Morozumi, C. Nitrogen pollution is linked to US listed species declines. *BioScience* **2016**, *66* (3), 213-  
451 222.
- 452 (20) Fu, X.; Wang, S.; Xing, J.; Zhang, X.; Wang, T.; Hao, J. Increasing ammonia concentrations reduce  
453 the effectiveness of particle pollution control achieved via SO<sub>2</sub> and NO<sub>x</sub> emissions reduction in East China.  
454 *Environ. Sci. Technol. Lett.* **2017**, *4* (6), 221-227.

- (21) Dong, W. X.; Xing, J.; Wang, S. X. Temporal and spatial distribution of anthropogenic ammonia emissions in China:1994-2006. *Environ. Sci.* **2010**, *31* (7), 1457-1463 (in Chinese).
- (22) Huang, X.; Song, Y.; Li, M.; Li, J.; Huo, Q.; Cai, X.; Zhu, T.; Hu, M.; Zhang, H. A high-resolution ammonia emission inventory in China. *Global Biogeochem. Cycles* **2012**, *26* (1), 239256.
- (23) Kang, Y.; Liu, M.; Song, Y.; Huang, X.; Yao, H.; Cai, X.; Zhang, H.; Kang, L.; Liu, X.; Yan, X.; et al. High-resolution ammonia emissions inventories in China from 1980 to 2012. *Atmos. Chem. Phys.* **2016**, *16* (4), 2043-2058.
- (24) Emissions Database for Global Atmospheric Research (EDGAR v4.3.1). <http://edgar.jrc.ec.europa.eu/overview.php?v=431> (accessed July 6, 2016).
- (25) Wang, S. W.; Liao, J. H.; Yu-Ting, H. U.; Yan, X. Y. A preliminary inventory of NH<sub>3</sub>-N emission and its temporal and spatial distribution of China. *J. Agro-Environ. Sci.* **2009**, *28* (3), 619-626 (in Chinese).
- (26) Kurokawa, J.; Ohara, T.; Morikawa, T.; Hanayama, S.; Janssens-Maenhout, G.; Fukui, T.; Kawashima, K.; Akimoto, H. Emissions of air pollutants and greenhouse gases over Asian regions during 2000–2008: Regional Emission inventory in Asia (REAS) version 2. *Atmos. Chem. Phys.* **2013**, *13* (21), 11019-11058.
- (27) Wang, G.; Zhang, R.; Gomez, M. E.; Yang, L.; Levy Zamora, M.; Hu, M.; Lin, Y.; Peng, J.; Guo, S.; Meng, J.; et al. Persistent sulfate formation from London Fog to Chinese haze. *Proc. Natl. Acad. Sci. U. S. A.* **2016**, *113* (48), 13630-13635.
- (28) Wu, Y.; Gu, B.; Erisman, J. W.; Reis, S.; Fang, Y.; Lu, X.; Zhang, X. PM<sub>2.5</sub> pollution is substantially affected by ammonia emissions in China. *Environ. Pollut.* **2016**, *218*, 86-94.
- (29) The National Bureau of statistics of the People's Republic of China; *China Statistical Yearbook (2001-2016)*; China Statistics Press: Beijing, China, 2016.
- (30) FAOStat: Food and Agriculture Data, Food and Agriculture Organization. <http://faostat3.fao.org/home/E> (accessed December 10, 2015).
- (31) Gu, B.; Ge, Y.; Ren, Y.; Xu, B.; Luo, W.; Jiang, H.; Gu, B.; Chang, J. Atmospheric Reactive Nitrogen in China: Sources, Recent Trends, and Damage Costs. *Environ. Sci. Technol.* **2012**, *46* (17), 9420-9427.
- (32) Sutton, M. A.; Reis, S.; Riddick, S. N.; Dragosits, U.; Nemitz, E.; Theobald, M. R.; Tang, Y. S.; Braban, C. F.; Vieno, M.; Dore, A. J.; et al. Towards a climate-dependent paradigm of ammonia emission and deposition. *Philos. Trans. R. Soc., B* **2013**, *368* (1621), 20130166.
- (33) Warner, J. X.; Dickerson, R. R.; Wei, Z.; Strow, L. L.; Wang, Y.; Liang, Q. Increased atmospheric ammonia over the world's major agricultural areas detected from space. *Geophys. Res. Lett.* **2017**, *44* (6), 2875-2884.
- (34) Meng, W.; Zhong, Q.; Yun, X.; Zhu, X.; Huang, T.; Shen, H.; Chen, Y.; Chen, H.; Zhou, F.; Liu, J.; et al. Improvement of a global high-resolution ammonia emission inventory for combustion and industrial sources with new data from the residential and transportation sectors. *Environ. Sci. Technol.* **2017**, *51* (5), 2821-2829.
- (35) Xu, P.; Liao, Y. J.; Lin, Y. H.; Zhao, C. X.; Yan, C. H.; Cao, M. N.; Wang, G. S.; Luan, S. J. High-resolution inventory of ammonia emissions from agricultural fertilizer in China from 1978 to 2008. *Atmos. Chem. Phys.* **2016**, *16* (3), 1207-1218.
- (36) Xu, P.; Zhang, Y. S.; Gong, W. W.; Hou, X. K.; Kroeze, C.; Gao, W.; Luan, S. J. An inventory of the emission of ammonia from agricultural fertilizer application in China for 2010 and its high-resolution spatial distribution. *Atmos. Environ.* **2015**, *115*, 141-148.
- (37) Liu, F.; Zhang, Q.; van DerA, R. J.; Zheng, B.; Tong, D.; Yan, L.; Zheng, Y.; He, K. Recent reduction in NO<sub>x</sub> emissions over China: synthesis of satellite observations and emission inventories. *Environ. Res.*

- 498 *Lett.* **2016**, *2016* (11), 114002.
- 499 (38) Clarisse, L.; Clerbaux, C.; Dentener, F.; Hurtmans, D.; Coheur, P. Global ammonia distribution derived  
500 from infrared satellite observations. *Nature Geosci.* **2009**, *2* (7), 479-483.
- 501 (39) Van Damme, M.; Erisman, J. W.; Clarisse, L.; Dammers, E.; Whitburn, S.; Clerbaux, C.; Dolman, A.  
502 J.; Coheur, P. F. Worldwide spatiotemporal atmospheric ammonia (NH<sub>3</sub>) columns variability revealed by  
503 satellite. *Geophys. Res. Lett.* **2015**, *42* (20), 8660-8668.
- 504 (40) Whitburn, S.; Van Damme, M.; Clarisse, L.; Bauduin, S.; Heald, C. L.; Hadji-Lazaro, J.; Hurtmans,  
505 D.; Zondlo, M. A.; Clerbaux, C.; Coheur, P. F. A flexible and robust neural network IASI-NH<sub>3</sub> retrieval  
506 algorithm. *J. Geophys. Res. Atmos.* **2016**, *121* (11), 6581-6599.
- 507 (41) Liu, L.; Zhang, X.; Xu, W.; Liu, X.; Lu, X.; Wang, S.; Zhang, W.; Zhao, L. Ground Ammonia  
508 Concentrations over China Derived from Satellite and Atmospheric Transport Modeling. *Remote Sens.*  
509 **2017**, *9* (5), 467.
- 510 (42) Zhang, Y.; Luan, S.; Chen, L.; Shao, M. Estimating the volatilization of ammonia from synthetic  
511 nitrogenous fertilizers used in China. *J. Environ. Manage.* **2011**, *92* (3), 480-493.
- 512 (43) Wang, J. Q.; Wen-Qi, M. A.; Jiang, R. F.; Zhang, F. S. Analysis about amount and ratio of basal  
513 fertilizer and topdressing fertilizer on rice, wheat, maize in China. *Chin. J. Soil Sci.* **2008**, *39* (2), 329-333  
514 (in Chinese).
- 515 (44) Fu, X.; Wang, S. X.; Ran, L. M.; Pleim, J. E.; Cooter, E.; Bash, J. O.; Benson, V.; Hao, J. M. Estimating  
516 NH<sub>3</sub> emissions from agricultural fertilizer application in China using the bi-directional CMAQ model  
517 coupled to an agro-ecosystem model. *Atmos. Chem. Phys.* **2015**, *15* (12), 6637-6649.
- 518 (45) Pan, B.; Lam, S. K.; Mosier, A.; Luo, Y.; Chen, D. Ammonia volatilization from synthetic fertilizers  
519 and its mitigation strategies: A global synthesis. *Agric., Eco. & Environ.* **2016**, *232*, 283-289.
- 520 (46) Ju, X.; Gu, B.; Wu, Y.; Galloway, J. N. Reducing China's fertilizer use by increasing farm size. *Global*  
521 *Environ. Chang.* **2016**, *41*, 26-32.
- 522 (47) Bai, Z. H.; Ma, L.; Qin, W.; Chen, Q.; Oenema, O.; Zhang, F. S. Changes in Pig Production in China  
523 and Their Effects on Nitrogen and Phosphorus Use and Losses. *Environ. Sci. Technol.* **2014**, *48* (21), 12742-  
524 12749.
- 525 (48) Fu, X.; Wang, S. X.; Ran, L. M.; Pleim, J. E.; Cooter, E.; Bash, J. O.; Benson, V.; Hao, J. M. Estimating  
526 NH<sub>3</sub> emissions from agricultural fertilizer application in China using the bi-directional CMAQ model  
527 coupled to an agro-ecosystem model. *Atmos. Chem. Phys.* **2015**, *15* (12), 6637-6649.
- 528 (49) Bai, Z.; Ma, L.; Jin, S.; Ma, W.; Velthof, G. L.; Oenema, O.; Liu, L.; Chadwick, D.; Zhang, F. Nitrogen,  
529 Phosphorus, and Potassium Flows through the Manure Management Chain in China. *Environ. Sci. Technol.*  
530 **2016**, *50* (24), 13409-13418.
- 531 (50) Jia, Y.; Yu, G.; Gao, Y.; He, N.; Wang, Q.; Jiao, C.; Zuo, Y. Global inorganic nitrogen dry deposition  
532 inferred from ground- and space-based measurements. *Sci. Rep.* **2016**, *6* (19810), 1-11.
- 533 (51) Jia, Y.; Yu, G.; He, N.; Zhan, X.; Fang, H.; Sheng, W.; Zuo, Y.; Zhang, D.; Wang, Q. Spatial and  
534 decadal variations in inorganic nitrogen wet deposition in China induced by human activity. *Sci. Rep.* **2014**,  
535 *4* (3763), 1-7.
- 536 (52) Zhu, J.; He, N.; Wang, Q.; Yuan, G.; Wen, D.; Yu, G.; Jia, Y. The composition, spatial patterns, and  
537 influencing factors of atmospheric wet nitrogen deposition in Chinese terrestrial ecosystems. *Sci. Total.*  
538 *Environ.* **2015**, *2015* (511), 777-785.
- 539 (53) Van Damme, M.; Whitburn, S.; Clarisse, L.; Clerbaux, C.; Hurtmans, D.; Coheur, P. F. Version 2 of  
540 the IASI NH<sub>3</sub> neural network retrieval algorithm; near-real time and reanalysed datasets. *Atmos. Meas.*

541 *Tech. Disc.* **2017**, doi:10.5194/amt-2017-239.  
542 (54) China statistical yearbook on environment (2001-2015). <http://datacenter.mep.gov.cn>.  
543 .  
544  
545

**Table 1 N input, NH<sub>3</sub> emission and deposition in the world and China**

	World			China
	1860 <sup>a</sup>	early-1990s <sup>a</sup>	2010 <sup>b</sup>	2010 <sup>c</sup>
<b>Total terrestrial N input</b>	<b>135</b>	<b>263</b>	<b>278</b>	<b>61.3</b>
Fertilizer production	0	100	120	37.1
NBNF	120	107	58	7.1
CBNF	15	31.5	60	4.6
NO <sub>x</sub> -FF	0.3	24.5	40	6.6
<b>NH<sub>3</sub> emission</b>	<b>20.5</b>	<b>58.2</b>	<b>69</b>	<b>14.0</b>
Terrestrial	14.9	52.6	60	14.0
Marine	5.6	5.6	9	-
<b>NH<sub>x</sub> deposition</b>	<b>18.8</b>	<b>56.7</b>	<b>64</b>	<b>13.8</b>
Terrestrial	10.8	38.7	40	13.1 <sup>d</sup>
Marine	8	18	24	0.7 <sup>e</sup>

Unit: Tg N yr<sup>-1</sup>; Fertilizer production, Haber–Bosch N fixation for fertilizer use; NBNF, natural biological N fixation; CBNF, cultivated biological N fixation; NO<sub>x</sub>-FF, NO<sub>x</sub> emission via fossil fuel combustion.

a, adapted from Galloway et al.<sup>8</sup>

b, adapted from Fowler et al.<sup>2</sup>

c, adapted from Gu et al.<sup>7</sup>

d, adapted from Liu et al.<sup>17</sup>

e, adapted from Luo et al.<sup>10</sup>

**Table 2 NH<sub>x</sub> deposition on land area of China.**

Studies	Base year	Deposition density (kg N ha <sup>-1</sup> yr <sup>-1</sup> )			Total deposition (Tg N yr <sup>-1</sup> )
		Dry	Wet	Total	
Jia et al. <sup>50, 51</sup>	2000-2009	-	-	13.9	12.9
Liu et al. <sup>17</sup>	2000-2010	-	-	14.3	13.3
Xu et al. <sup>6</sup>	2010-2014	-	-	14.5	13.5
Liu et al. <sup>18</sup>	2003-2014	-	6.8	-	6.3*
Jia et al. <sup>51</sup>	2005-2014	6.1	-	-	5.7*
Zhu et al. <sup>52</sup>	2013	-	7.3	-	6.8*

\* Only wet or dry NH<sub>x</sub> deposition.

**Table 3 Comparison of NH<sub>3</sub> emissions with other studies**

Studies	Year	Total	Fertilizer	Livestock	Humans	Burning	Others
REAS	2000	10.3 // +1.8	4.2 // -0.2	4.2 // +0.9	1.2 // -0.1	0.5 // -0.3	0.2 // +1.4
Wang et al.	2005	13.4 // -0.2	4.2 // +0.1	5.8 // -0.1	0.2 // +0.8	-	3.3 // -1.2
Huang et al.	2006	8.1 // +5.1	2.6 // +2.1	4.4 // +1.3	0.2 // +0.7	0.1 // +0.2	0.8 // +0.8
Dong et al.	2006	13.2 // +0.1	7.2 // -2.5	5.4 // +0.3	0.5 // +0.4	-	0.1 // +1.8
Paulot et al.	2007	8.4 // +5.1	3.0 // +1.9	4.8 // +0.9	-	-	0.6 // +2.3
Xu et al.	2008	-	2.7 // +2.0	3.1 // +2.8	0.6 // +0.3	-	-
EDGAR	2010	11.5 // +2.3	4.9 // -0.1	4.2 // +1.9	-	-	0.7 // +2.4
Xu et al.	2010	-	3.7 // +1.2	4.2 // +2.0	0.4 // +0.4	-	-
Fu et al.	2011	-	2.5 // +2.3	-	-	-	-
Kang et al.	2012	8.0 // +6.7	2.3 // +2.7	4.1 // +2.4	0.1 // +0.7	0.3 // -0.1	1.1 // +1.1

Note that before the “//” is the previous studies, after the “//” is the difference of our result with previous studies, +xx or -yy in red/green colors in each column represents higher or lower value in our study than previous research; “-” means unavailable data; all the units of NH<sub>3</sub> emission have been converted to the Tg N yr<sup>-1</sup>.

REAS <sup>26</sup>

Wang et al. <sup>25</sup>

Huang et al. <sup>22</sup>

Dong et al. <sup>21</sup>

Paulot et al. <sup>16</sup>

Xu et al. <sup>35</sup>

EDGAR <sup>24</sup>

Xu et al. <sup>36</sup>

Fu et al. <sup>44</sup>

Kang et al. <sup>23</sup>

**Figure Legend**

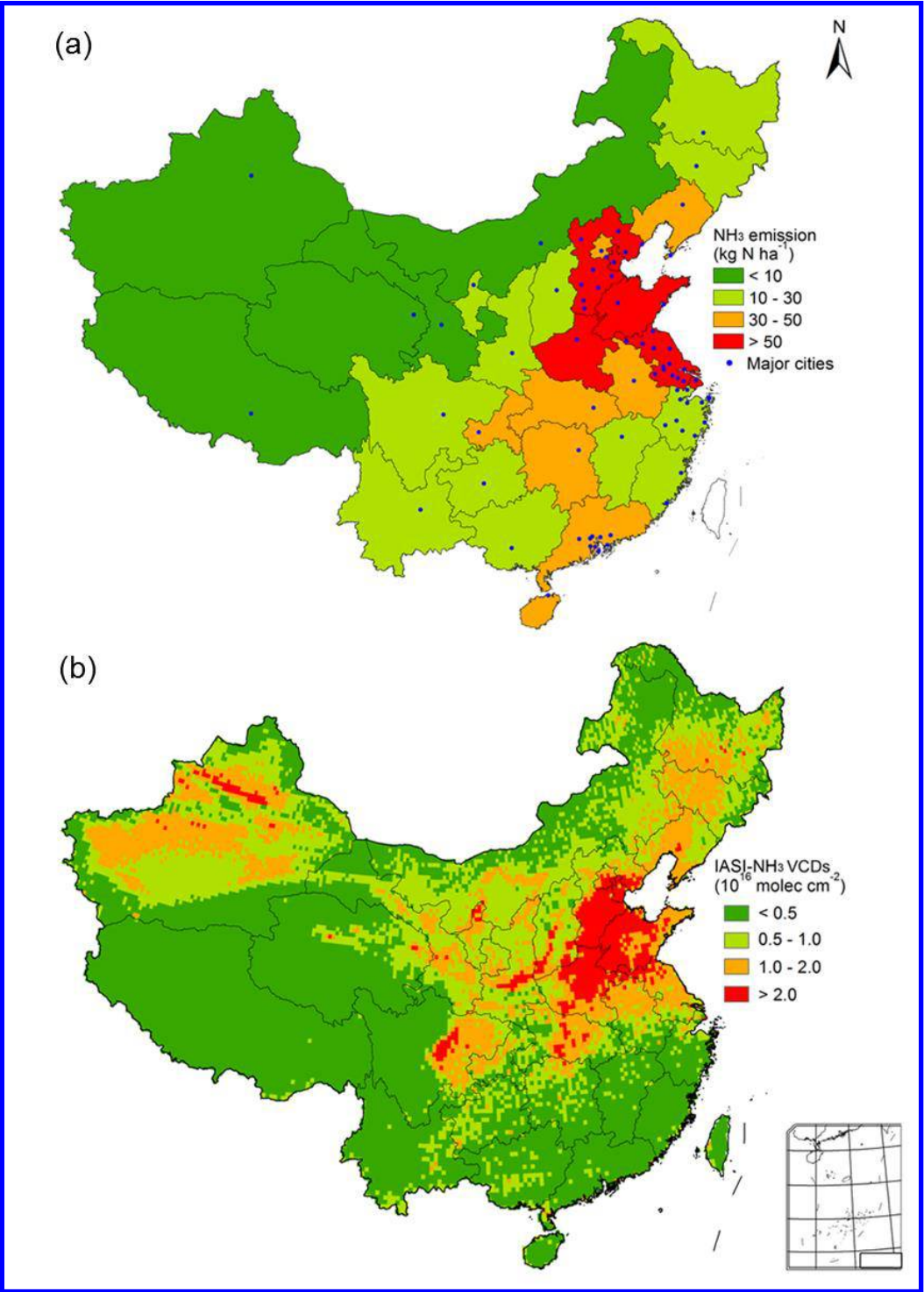
**Figure 1 Validation by satellite observations (IASI) on spatial patterns.** (a) The spatial patterns of  $\text{NH}_3$  emission density in mainland China in 2015; (b) Mean IASI- $\text{NH}_3$  VCDs ( $10^{16}$  molec  $\text{cm}^{-2}$ ) distribution for 2015 over China. Data of  $\text{NH}_3$  VCDs are derived from an improved version of the IASI dataset presented in Whitburn et al.<sup>40</sup> and Van Damme et al.<sup>53</sup>

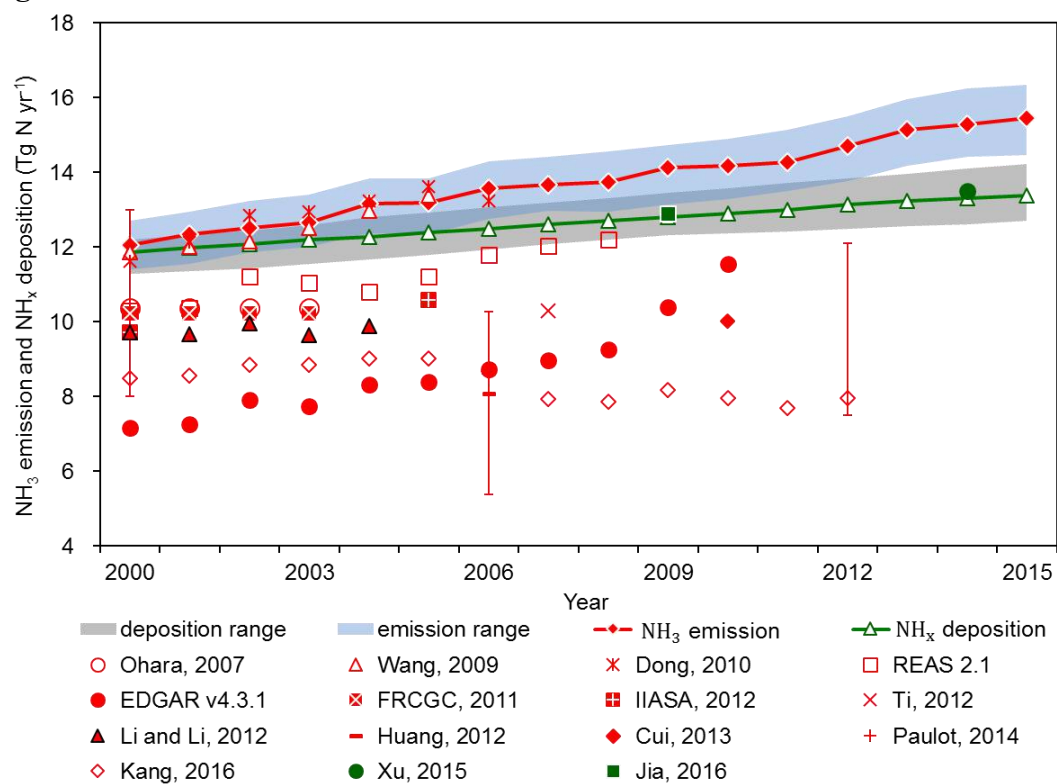
**Figure 2 Comparison of  $\text{NH}_3$  emissions with other published results and  $\text{NH}_x$  deposition in mainland China during 2000-2015.** Studies addressing  $\text{NH}_3$  emissions are colored with red symbols and  $\text{NH}_x$  deposition colored with green symbols (references presented in this figure are listed in the SI TextS4). The red dotted line represents the  $\text{NH}_3$  emission estimated in this study, and the green dotted line represents the  $\text{NH}_x$  deposition synthesized by this study. The blue and grey shaded area indicates the 95% confidence interval of  $\text{NH}_3$  emission evaluated by our study and  $\text{NH}_x$  deposition on land calculated using data provided by Liu et al.<sup>17</sup> and Xu et al.<sup>6</sup>, respectively. Error bars of the symbols represent the uncertainties of their estimates, those symbols without error bars mean uncertainties unavailable or yet been discussed.

**Figure 3 Comparison with  $\text{SO}_2$  &  $\text{NO}_x$  emission on temporal trends.** The two solid lines show the molar ratios of  $(2\text{SO}_2 + \text{NO}_x)/\text{NH}_3$  and  $2\text{SO}_2/\text{NH}_3$  in 2000-2015 in China. The dash line represents the molar ratio = 1. A ratio  $>1$  represents  $\text{NH}_3$  limitation to form the ammonium aerosol. While a ratio  $<1$  represents  $\text{NH}_3$  is available in abundance to form the ammonium aerosol contributing to Secondary Inorganic Aerosol formation (SIA), a substantial contributor to  $\text{PM}_{2.5}$  concentrations. Data of  $\text{SO}_2$ ,  $\text{NO}_x$  and  $\text{NH}_3$  emission is based on MEPC,<sup>54</sup> Liu et al.<sup>37</sup> and our study, respectively.

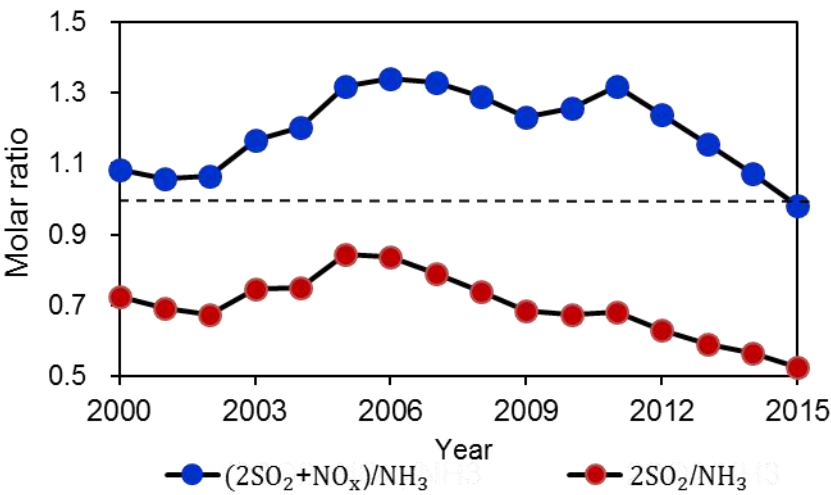
**Figure 4 Validation by satellite observations (AIRS) on temporal trends.** The AIRS- $\text{NH}_3$  VCDs at 918 hPa from 2003 to 2015 are showed in pink dashed curves, with linear fits in solid lines. Data for AIRS- $\text{NH}_3$  VCDs was extracted from Warner et al.<sup>33</sup> and Van Damme et al.<sup>53</sup> The green dotted line represents the  $\text{NH}_3$  emission estimated in this study.

Figure 1



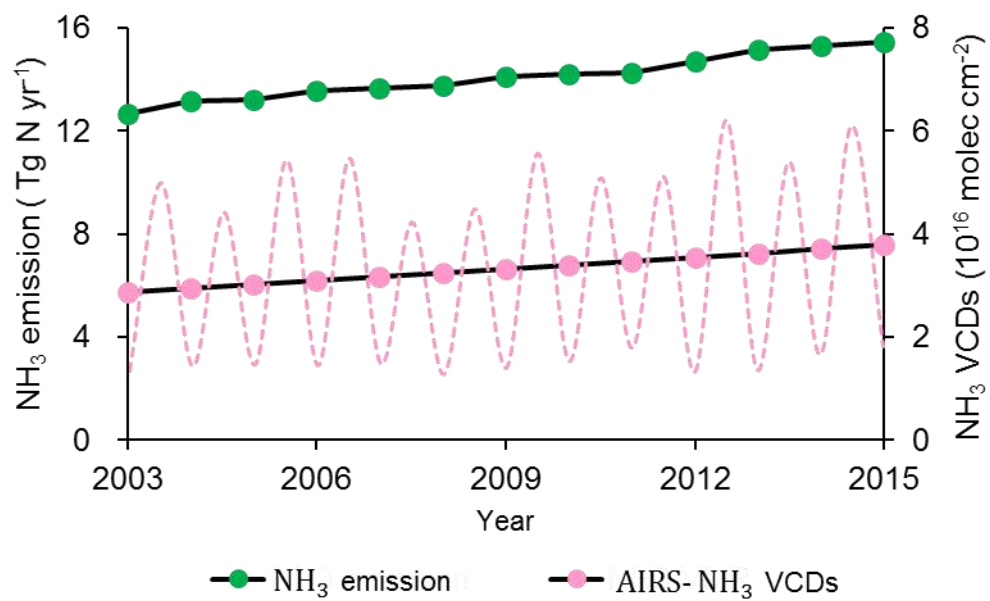
**Figure 2**

615     **Figure 3**



616

617

618 **Figure 4**

619

620

